Astron. Astrophys. 333, 665–672 (1998)

ASTRONOMY
AND
ASTROPHYSICS

The gallium problem in HgMn stars

M.M. Dworetsky⋆, C.M. Jomaron, and Claire A. Smith

Department of Physics and Astronomy, University College London, Gower Street, London WC1E 6BT, UK

Received 19 September 1997 / Accepted 15 January 1998

Abstract. Previous studies of visible-region high-excitation lines of Ga II in HgMn stars have usually concluded that these lines ($\lambda\lambda$4251-4262 and λ6334) yield abundance estimates for gallium $\sim$1 dex greater than the UV resonance lines. Of the explanations proposed in the literature, we find that the presence of hyperfine structure (hfs) in the lines is the most likely. We analyse Lick Hamilton Échelle CCD spectra by spectrum synthesis with the code UCLSYN. Using the Bidelman & Corliss (1962) measurements of hfs in Ga II, and the calculations given by Lanz et al. (1993), with the oscillator strengths by Ryabchikova & Smirnov (1994), we determine a difference in abundance (visual-UV) of only 0.2 dex. Of this difference, about 0.1 dex can be explained by the simplified approximation to the true hfs, which can be estimated theoretically, and the remaining 0.1 dex can probably be accounted for by the stratification of Ga found by Smith (1995, 1996b). We conclude that the visible-region and UV abundances are in agreement within the errors of the determinations, and that the anomaly previously found by several investigations is an artifact of the simplified atomic line structures assumed, or results from the use of very different *gf*–values from those adopted here.

Key words: stars: abundances – stars: chemically peculiar – stars: rotation – atomic data

1. Introduction

The HgMn stars are considered by many researchers a nearly ideal natural laboratory in which to study the effects of radiative diffusion and gravitational settling in relatively quiescent stellar atmospheres without complications due to rapid rotation, high microturbulence and strong magnetic fields (Vauclair & Vauclair 1982; Smith 1996b). They may also be useful in estimating atomic data (Lanz 1995). During the evolution of such stars, their surface abundances change in striking ways, leading to abundance enhancements of some rare elements by factors of 10^{3-4}, and to more subtle anomalies in many of the more abundant elements (Smith & Dworetsky 1993; Smith 1996b). One of the best-known and well-studied anomalies in these stars is the strong overabundance of the rare element gallium (Z = 31). The story of the discovery and analysis of Ga II in optical spectra of HgMn and related stars dates from the work of Bidelman in 1960, as reported by Jugaku et al (1961) and Bidelman & Corliss (1962).

Authors of several recent studies of abundances in HgMn stars have commented on the apparently intractable $\sim$1 dex difference in the abundance of gallium deduced from the UV resonance transitions of Ga II and Ga III and that deduced from the high-excitation ($E_i \sim 13 - 14$ eV) lines seen in the visible region of the spectrum (Lanz et al. 1993; Ryabchikova & Smirnov 1994; Smith 1995; Smith 1996a). This is especially noticeable in stars with the highest UV Ga abundances (Takada-Hidai et al. 1986, their Table 4). Lanz et al. considered the effects of hyperfine structure on λ6334 (4s5s ^{3}S$_1$–4s5p ^{3}P$^\circ_2$) in detail, but concluded that the LTE abundance difference deduced from red and ultraviolet transitions remained ~ 1 dex, with the UV observations consistently giving the lower abundance. Ryabchikova & Smirnov considered both the 4d ^{3}D–4f ^{3}F and 4d ^{3}D–4f ^{1}F ($\lambda\lambda$4250–4262) and the λ6334 lines with revised oscillator strengths and concluded again that there was an abundance difference in κ Cnc of more than an order of magnitude between their results and those of Takada-Hidai et al. (1986) in the UV. Although Adelman (1992, 1994) did not comment directly on the UV-visible difference, the Ga abundances given in his papers and in Ryabchikova et al. (1996) lend support to claims of a difference which ranges up to $\sim$ 1 dex in the stars with the strongest lines. These data suggest that the difference falls to ~ 0.3 dex in stars with detected but weak Ga II lines.

Smith (1995) re-examined the problem of the derivation of Ga abundances from the UV resonance lines of Ga II and Ga III and demonstrated that Ga II λ1495 shows an anomaly in its profile when analysed under the assumptions of LTE and homogeneous abundance with depth, but that this anomaly is removed when one relaxes the assumption of homogeneity and allows Ga to be concentrated in a cloud with a lower base around $\log \tau_{\rm lower} \sim 0.0$ and an upper bound around -3 ($\tau = \tau_{5000}$). He also considered whether his stratification model could account for the difference between the UV and visual-region abundance results and concluded that it cannot. In a second paper on the abundances of Ga from IUE observations of HgMn stars (Smith 1996a), he demonstrated that stratification could not account for

Send offprint requests to: M.M. Dworetsky (mmd@star.ucl.ac.uk)
⋆ Guest Observer, Lick Observatory

differences of more than ~ 0.1 dex, which falls far short of the discrepancy.

It would help to give a name to this stubborn anomaly; let us call it "The Gallium Problem." It is the reported difference of about 1 dex between abundances for Ga derived from UV resonance lines and from visual wavelength features. Explanations offered include stratification effects, which according to Smith's investigations cannot be the cause; non-LTE effects, for which no calculations have yet been done; and the neglect of hyperfine structure, as suggested by Smith (1996a), although Lanz et al. included it explicitly yet the Gallium Problem remained.

In this paper we follow Smith's suggestion by analysing our CCD échelle spectra of the HgMn stars of the Smith & Dworetsky (1993) sample under the assumption that hyperfine structure in the $\lambda\lambda$4250-4262 and λ6334 lines needs to be modelled explicitly, in order to see if it could account for the Gallium Problem and resolve it without resort to any other explanation. We show (once a further allowance is made for blending features) that this is indeed the case. Ryabchikova & Smirnov–in a note added in proof to their paper–have already suggested that the reason that Lanz et al. (1993) did not reach a similar conclusion was due to their use of a much smaller *gf*–value. We find that the mean difference between UV and visible abundances is around 0.2 dex, well within the range of explanation by a combination of different sources of atomic data, errors in the UV analyses, minor inadequacies of our simple line models, and the stratification effects on the lines described by Smith (1996a).

Table 1. Stellar parameters[a]

Star	HD	$T_{\rm eff}$ (K)	$\log g$ (cm s^{-2})	ξ^b	$v \sin i^b$
87 Psc	7374	13 150	4.00	1.5	21.0
53 Tau	27295	12 000	4.25	0.0	6.5
μ Lep	33904	12 800	3.85	0.0	15.5
HR 1800	35548	11 050	3.80	0.5	3.0
33 Gem	49606	14 400	3.85	0.5	22.0
HR 2676	53929	14 050	3.60	1.0	25.0
HR 2844	58661	13 460	3.80	0.5	27.0
κ Cnc	78316	13 500	3.80	0.0	7.0
36 Lyn	79158	13 700	3.65	2.0	49.0
υ Her	144206	12 000	3.80	0.6	9.0
ϕ Her	145389	11 650	4.00	0.4	10.1
28 Her	149121	11 000	3.80	0.0	10.0
HR 6997	172044	14 500	3.90	1.5	36.0
112 Her	174933	13 100	4.10	0.0	5.5
HR 7143	175640	12 100	4.00	1.0	2.0
HR 7361	182308	13 650	3.55	0.0	8.2
46 Aql	186122	13 000	3.65	0.0	3.0
HR 7664	190229	13 200	3.60	0.8	8.0
HR 7775	193452	10 800	3.95	0.0	0.0
β Scl	221507	12 400	3.90	0.0	25.0

[a] All parameters except $v \sin i$ and those for 112 Her are from Smith & Dworetsky (1993), whose $v \sin i$ values were revised during this analysis. Parameters for 112 Her from Ryabchikova et al. (1996)
[b] km s^{-1}

2. Observations

The list of observed objects is given in Table 1. These include nearly all the HgMn stars of the original Smith & Dworetsky (1993) IUE sample of normal, superficially-normal, and HgMn stars. We observed with the Hamilton Échelle Spectrograph (HES; Vogt 1987, Misch 1997) at Lick Observatory, fed by the 0.6-m Coudé Auxilliary Telescope (CAT), during runs in November-December 1994, July 1995, May 1996, and May 1997. The only objects not observed were κ Cep (too far north for the CAT) and stars south of -35°. Of the latter, all except HR 6000 were observed (in the blue region only) for us by service observations at the Anglo-Australian Telescope (AAT) using the UCL Échelle spectrograph. Shortly before our observations in 1994, some of the HES optical components were replaced, improving the resolution and instrumental profile, and making it possible to use the full field of the 2048 $\times$ 2048 CCDs to maximum advantage. We used both the unthinned phosphor-coated Orbit CCD (Dewar 13) and the thinned Ford CCD (Dewar 6), depending on availability as the latter is shared with the multi-object spectrograph on the 3-meter telescope. The spectral range for the observations was 3800–9000 Å except for the AAT data which was only obtained in the range 3700–4700 Å with the TEK2 CCD. Typical S/N per pixel in the centers of orders ranged from 75 to 250. The Orbit CCD is cosmetically very clean, with very few bad pixels or columns, while the thinned Ford CCD contains several column defects but offers a much higher detector quantum efficiency in the blue. We used the Ford CCD whenever it was available. It also has excellent flatness characteristics as evidenced by mapping during focus settings (Misch 1995). With the slit settings used, the combination of spectrographs and CCDs gave resolutions $R \approx 46\,500$ for the HES, and slightly less ($\sim 44\,000$) for the UCLES. Flat fields were made using polar axis quartz lamps and wavelength calibrations were obtained with Th–Ar comparisons.

The échelle spectra were extracted and calibrated using standard IRAF extraction packages (Churchill 1995; Valdes 1990). Earlier measurements (Allen 1997) showed that there were no measurable effects of parasitic light (scattered light) in the line profiles provided that general scattered light in the adjacent interorder spaces was taken as the subtracted background. In practice this means that scattered light was less than about 1 percent. Some examples of unmerged single-order spectra of κ Cnc are shown in Figs. 2-6.

3. Atomic data

The four Ga II lines in the 4250–4262Å region were observed in the laboratory with very high resolution (dispersion 0.86 Åmm^{-1}) by Bidelman & Corliss (1962). They detected structure and hyperfine blurring in three of the four lines, which, as they commented, contributed to the confirmation of the identification of the somewhat fuzzy stellar features in 3 Cen, κ Cnc, and 112 Her. Following a suggestion by Guthrie (1984), we model our blue Ga II lines on their observations, using their wavelengths and taking as few liberties as possible with their

Table 2. Adopted model lines

Wavelength	Excitation Potential	log *gf*
4251.108	14.11	−0.33
4251.156	14.11	0.25
4254.032	14.11	−0.70
4254.082	14.11	−0.41
4255.640	14.11	0.00
4255.704	14.11	0.10
4255.768	14.11	0.40
4255.902	14.11	−0.30
4261.995	14.12	0.98

data in doing so. The study of the spectrum of Ga II by Isberg & Litzén (1985) provided data for a wide range of wavelengths, but with much lower dispersion (5 Åmm^{-1} in the blue). We add a fifth, weak transition at 4255.902Å not reported by Bidelman & Corliss but observed by Isberg & Litzén (1985) at 4255.92 Å; we adopt a wavelength appropriate to its calculated wavenumber difference rather than the reported wavelength as this gives more precision for this weak feature and the resulting fits to the stellar observations of the stronger adjacent line are improved as a result.

Oscillator strengths for the four lines are taken from the branching ratios of Ryabchikova & Smirnov (1994; their Table 1). They employed beam-foil lifetimes measured by Andersen & Sørensen (1972). Three of their *gf*–values agree, within 0.1–0.2 dex, with the Bates & Damgaard (1949) calculations of Jugaku et al. (1961); the other line, λ4254, an intercombination line, was not reported in that paper. We derive our simplified models for the hfs of the lines as follows: for λ4251, λ4255, and λ4262, we adopt the component wavelengths given by Bidelman & Corliss and their component laboratory intensities, and divide the total *gf*–value of each line among its components assuming a linear intensity scale. The weak Ga feature at 4255.902 Å mentioned above is treated as a blend with a log *gf* = −0.30 crudely appropriate to its given intensity. For λ4254, we simulate the reported unresolved hfs (hazy, shaded longward) by arbitrarily assuming two components with an intensity ratio of 1:2 separated by 0.050 Å with a mean wavelength which best fit the stellar observations (4254.065 Å; compare 4254.075 by Isberg & Litzén and 4254.04 by Bidelman & Corliss). Our models for the blue Ga II lines are summarized in Table 2.

For the strongest red line of Ga II, λ6334, we adopt the calculated structure and relative intensities of hfs components given by Lanz et al. (1993). These authors gave *gf* = 2.29 from a calculation with intermediate coupling and some configuration interactions. There are no experimental lifetimes in the literature, so Ryabchikova & Smirnov estimated the lifetime for the upper level for λ6334 by extrapolating measured lifetimes for the same levels in the analogues of Ga II, namely In II and Tl II. They derived *gf* = 10.0. We adopt their estimate and divide it among the components according to their relative intensities. Clearly, this implies that we should derive abundances 0.64 dex smaller from this line than did Lanz et al., but the situation is not satisfactory as there exists no direct measurement of the oscillator strength of this line. Conclusions based on this line should be regarded as preliminary until the question of the correct *gf*–value is settled.

The damping parameter for each line is calculated as the sum of radiative, Stark, and Van der Waals damping constants at each optical depth in the model atmosphere throughout the line forming region. For the four blue Ga II lines, we adopt $\Gamma_R = 13.5\Gamma_{cl}$ based on the measured lifetimes of the upper and lower levels and for the red line, $\Gamma_R = 22\Gamma_{cl}$ (Ryabchikova & Smirnov; Ansbacher et al. 1985). For Stark broadening we use the calculations of Dimitrijević & Artru (1986); for λ4254 and λ6334, not included in their work, we use the approximate formulae of Griem (1968) for ions with modifications described by Cugier & Hardorp (1988), and with Gaunt factor approximations as implemented in UCLSYN (Smith 1992). Van der Waals broadening is expected to be small; we adopt the approximation given, e.g., by Warner (1967, eqns 2, 4, 6 and 7) when the upper and lower angular momentum quantum numbers are known. The final abundances are insensitive to the precise values of the damping parameters; we find that $\Delta \log A(\mathrm{Ga}) \leq 0.05$ if the adopted values are varied by a factor of 2.

4. Abundance analysis for Ga II

Only in those stars with very high abundances of Ga can the visible-region lines be detected and identified with certainty. We assumed an arbitrary lower limit of ∼5 mÅ for the strongest optical Ga II feature, λ4255, and calculated the threshold abundances for detection assuming $\log g = 4.0$. The limit for detection (∼ 5.0–5.5) is plotted as a function of $T_{\rm eff}$ in Fig. 1 along with the mean optical abundances (or upper limits) deduced for each programme star in Table 1. (Throughout this paper we refer to abundances in logarithmic units where $\log A(\mathrm{H}) = 12.00$.)

The previously published abundances (Smith 1996a) in the spectroscopic binaries HR 4072, χ Lup and ι CrB and the southern hemisphere star ϕ Phe are all much lower than their respective limits and these stars have no discernible trace of Ga II in our optical spectra. We could only obtain upper limits in HR 1800, HR 2676, 28 Her and 46 Aql. Detections in 87 Psc, 53 Tau, 33 Gem and 36 Lyn were marginal, with the abundances obtained being around the threshold values; only the strongest of the five Ga II lines studied could be observed in these stars, and the reliability of these marginal detections is affected by $v \sin i$ and S/N of the individual stars and their spectrograms.

All abundances presented here were deduced by trial-and-error fits by eye of synthesized UCLSYN spectra to the observed spectra, taking into account known blends. UCLSYN is a spectrum-synthesis code developed at UCL by Smith & Dworetsky (1988) and Smith (1992), with an extension for binary star spectra, called BINSYN, coded by Smalley (1996). We adopt full-width half-maximum (fwhm) Gaussian instrumental profiles based on the resolution measured from our study of Th-

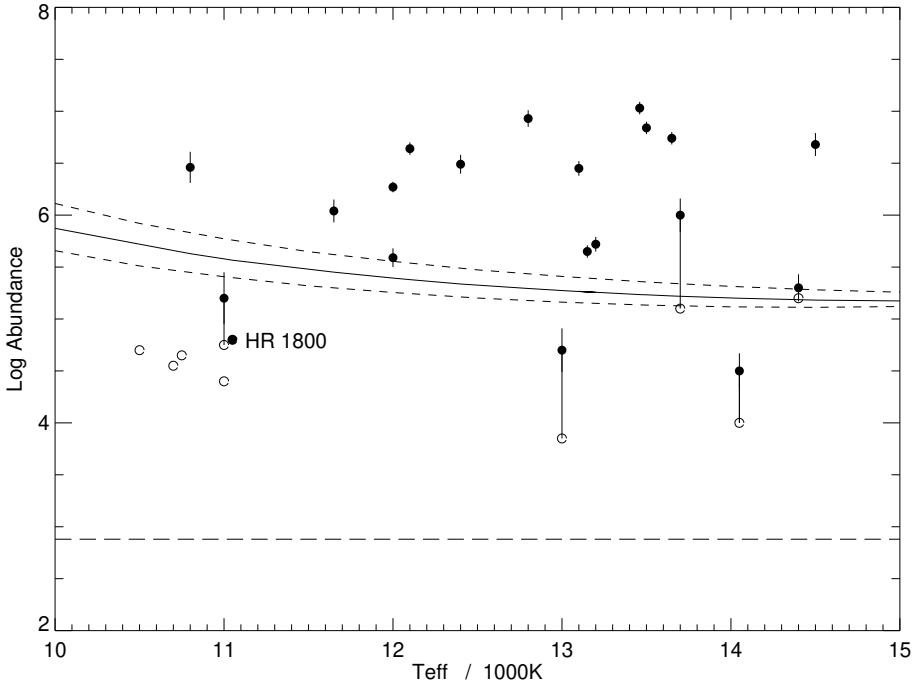

Fig. 1. Detection limit and mean Ga abundances. Filled circles: calculated mean Ga abundances for visible-region lines of Ga II. Open circles: UV abundances from Smith (1996a) for stars with Ga abundances below the detection limit. Upper limits are shown by filled circles being joined to unfilled circles (in the case of HR 1800, these two points coincide). The solid curve shows the detection limit (the abundance for a λ4255 equivalent width 5mÅ) at $\log g$ = 4.0. The dashed lines above and below this curve show this limit at $\log g$ of 4.5 and 3.5 respectively. The horizontal dashed line shows the solar Ga abundance ($\log A = 2.88$; Anders & Grevesse 1989). The four isolated unfilled circles represent the UV abundances of four stars not studied here because their Ga abundances are too low.

Ar arc lines taken during the Lick coudé observing runs, which consistently give $R \approx$46 500. The abundances for Fe, Cr and Mn listed in Smith & Dworetsky (1993) were used as starting points in the synthesis for separate unblended features and iterated until a fit was obtained. In this way a velocity correction was also obtained for each spectrum. The stellar parameters used are given in Table 1. Some of the $v \sin i$ values in Smith & Dworetsky (1993) were based on studies of lower dispersion photographic spectra of mixed quality. All of those values were checked and revised where required during synthesis of the Fe, Mn and Cr lines in order to give the best fit as judged from superimposed plots of synthetic and observed Lick coudé spectra. Thus the values for the stars listed in Table 1 supersede those earlier ones.

The main blending species for the four blue Ga II lines are Cr I and Cr II, Mn II, and to a lesser extent, Fe I and Fe II. In order to account consistently for Fe, Cr and Mn blends with the Ga lines, the log *gf* values of the blending lines given in the Kurucz (1990) CD23 list were adjusted in order to produce the same abundance for all lines of each element in those stars with low $v \sin i$ and low Ga abundance where the lines could be clearly seen. In this way, by fitting the lines of these species which remained unblended in stars with higher $v \sin i$ and high Ga abundances, we were able to account for the effects of the blends within the Ga II features. A similar exercise was carried out for the Ne I blend at λ6334, especially for the stars of highest $v \sin i$. The abundances deduced in this exercise have no special significance other than to allow us to reduce the number of free parameters in the Ga study, by fixing the strengths of individual blends in the syntheses.

The calculated abundances of gallium for each line synthesized are shown in Table 3. The individual lines are discussed below. An example of the synthesis fitted to the observations is shown in Figs. 2-6 which show the fits to the five lines for κ Cnc. The observed spectrum is shown as a histogram and the synthesized spectrum is shown as a solid line. The marks for Ga components are representative of their positions and approximate relative strengths, but for clarity the strengths of very weak components have been exaggerated.

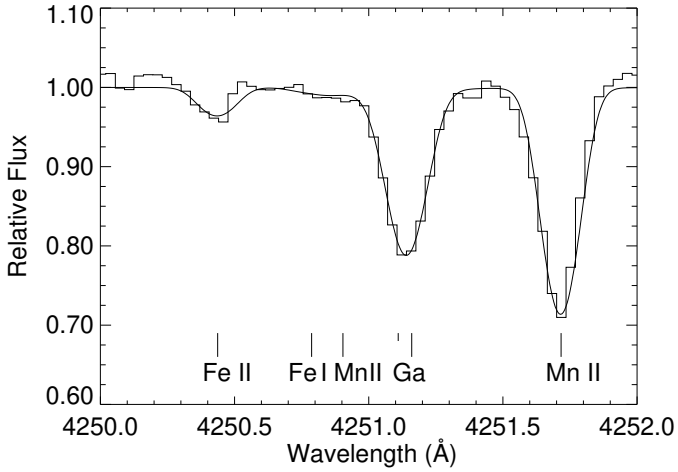

Fig. 2. Synthesis of the Ga λ4251 line in κ Cnc. The blends include the lines Fe II λ4250.437, Fe I λ4250.787, and Mn II λ4250.904 and λ4251.717. There is a cosmic-ray defect on part of Fe II λ4250.437.

4.1. Individual lines

– λ4251. The adopted hfs structure gives a good fit to this line in most of the stars studied. Potential blending lines are Fe II λ4250.437, Fe I λ4250.787 and Mn II λ4250.904, λ4251.717. It is relatively unblended in all but the stars with the greatest rotational broading and in those with very

Table 3. Gallium abundances

Star	Ga II Abundances (log N(H) = 12)					Mean	σ	Pub.
	λ4251	λ4254	λ4255	λ4262	λ6334			UV[a]
87 Psc	5.60	$\leq$6.0	5.55	5.80[b]	5.65	5.65	0.11	5.45
53 Tau	5.55	$\leq$5.7	5.60	5.40[b]	5.82	5.59	0.17	5.65
μ Lep	7.15	7.00	6.75	7.00[b]	6.75	6.93	0.18	6.50
HR 1800	$\leq$4.8	$\leq$4.8	$\leq$4.8	$\leq$4.8	$\leq$5.0	$\leq$4.8	0.09	4.80
33 Gem	5.60	$\leq$5.0	$\sim$5.3	$\leq$5.5	$\leq$5.0	$\leq$5.3	0.28	5.20
HR 2676	$\leq$4.3	$\leq$5.0	$\leq$4.3	$\leq$4.7	$\leq$4.0	$\leq$4.5	0.39	4.00
HR 2844	7.18	7.15	6.95	7.00[b]	6.85	7.03	0.14	6.75
κ Cnc	7.00	7.00	6.83	6.70	6.72	6.85	0.15	6.60
36 Lyn	$\leq$6.3	$\leq$6.5	$\leq$5.8	$\leq$5.7	5.80	$\leq$6.0	0.36	5.10
υ Her	6.43	6.32	6.14	6.25[b]	6.20	6.27	0.11	6.05
ϕ Her	6.22	$\sim$6.3	5.75	6.10[b]	5.82	6.04	0.24	5.70
28Her	$\leq$4.8	$\leq$6.1	$\leq$4.7	$\leq$5.2	$\leq$5.2	$\leq$5.2	0.55	4.75
HR 6997	6.82	7.00	6.68	6.50	6.40	6.68	0.24	6.45
112 Her	6.62	6.62	6.36	6.38	6.25	6.45	0.17	6.35
HR 7143	6.75	6.81	6.52	6.60[b]	6.51	6.64	0.14	6.35
HR 7361	6.90	6.87	6.66	6.70	6.58	6.74	0.14	6.35
46 Aql	$\leq$4.4	$\leq$5.5	$\leq$4.5	$\leq$4.6	$\leq$4.4	$\leq$4.7	0.47	3.85
HR 7664	5.85	5.90	5.70	5.55	5.60	5.72	0.15	5.60
HR 7775	6.66	6.73	6.38	6.65[b]	5.90	6.46	0.34	6.35
β Scl	6.55	6.70	6.35	6.35[b]	—	6.49	0.17	6.25
$\overline{\log(A/A_{\rm vis})}$	+0.12	+0.18	-0.09	-0.04	-0.15	—	—	-0.22

[a] Smith (1996a); [b] Ga II λ4262 badly blended with Cr II line.

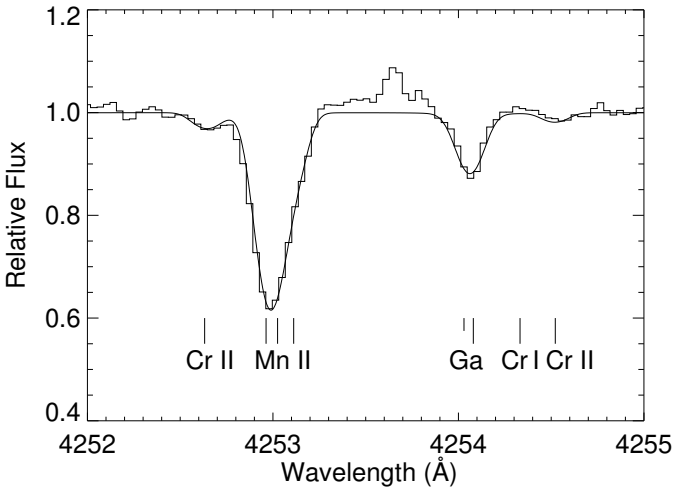

Fig. 3. Synthesis of the Ga λ4254 line in κ Cnc. The synthesis includes the lines Cr II λ4252.632 and λ4254.522, Cr I λ4254.332 and Mn II λ4252.963,λ4253.025 and λ4253.112. A wide cosmic-ray defect in the order shown does not seriously affect the Ga line.

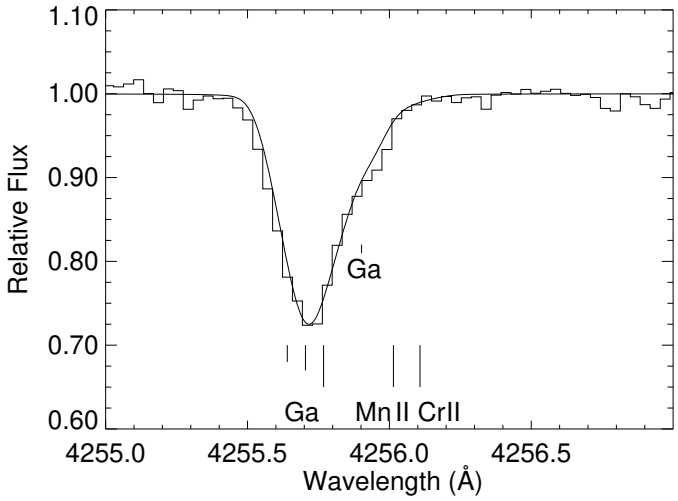

Fig. 4. Synthesis of the Ga λ4255 line in κ Cnc. The synthesis includes the weak lines Mn II λ4256.014 and Cr II λ4256.108.

high Fe or Mn abundances.

– λ4254. In a few cases this line is blended for the same reasons as discussed for the λ4251 line. The adopted hfs structure is our *ad hoc* fit to the slowest rotators. The blends are Cr I λ4254.332 and Cr II λ4254.522. The λ4254 line is the weakest of the four blue lines, hence for stars with near–threshold abundances of Ga this line was not observed.

– λ4255. This line is the strongest of the four blue lines and was blended to varying degrees in nearly all cases. The principal blends were Mn II λ4256.014 and Cr II λ4256.108. Again, the worst blending occurred for stars with relatively high $v \sin i$ and/or high abundances of the blending elements.

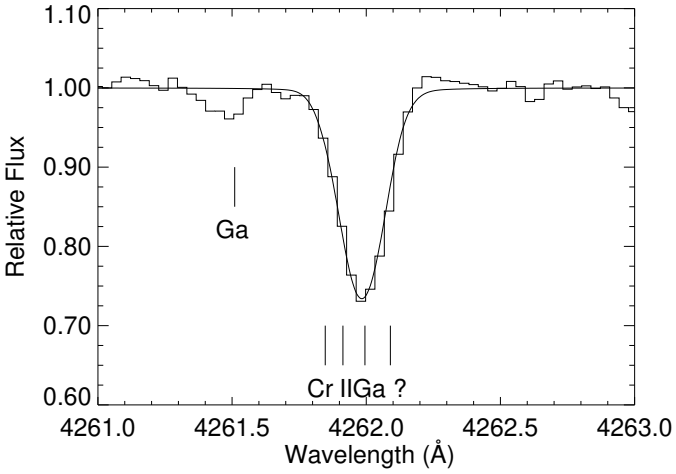

Fig. 5. Synthesis of the Ga λ4262 line in κ Cnc. The synthesis includes the lines Cr II λ4261.847 and λ4261.913 and the unknown blend at λ4262.090. We have not synthesized the weak Ga λ4261.51 line as it can only be seen in a few stars with the very strongest Ga lines and has no measured *gf*–value.

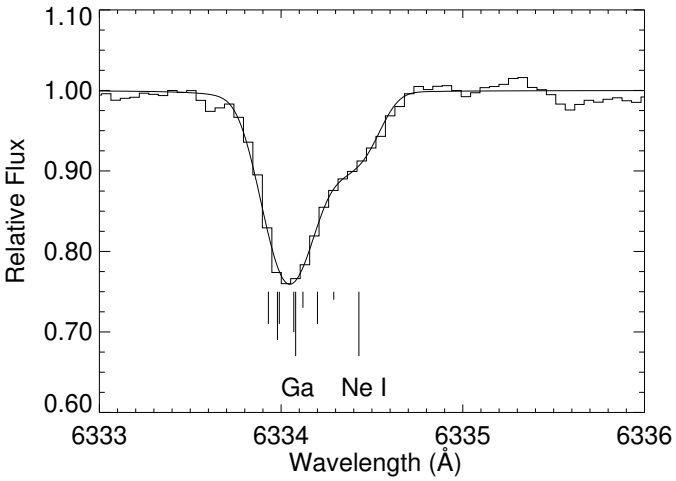

Fig. 6. Synthesis of the Ga λ6334 line in κ Cnc. The synthesis includes the line Ne I λ6334.428.

– λ4262. This line poses more of a problem as it is heavily blended in many stars with Cr II λ4261.847 and λ4261.913. In several stars it also shows a definite blend at λ4262.090 which could not be identified. No correlation of the observed unknown blend with the strength of Fe II, Cr II, or Mn II lines is found, indicating that the blend is due to some other element. The Kurucz (1990) CD23 line list does not contain any plausible candidates, and the line remains unidentified.

– λ6334. This is the strongest of the Ga II lines in the red part of the spectrum. In about half the stars studied this line shows a blend of varying strength with Ne I λ6334.428. We were generally able to allow completely for this blend in all except the stars with highest $v \sin i$.

Table 4. Equivalent widths

Star	Equivalent Widths (mÅ)				
	λ4251	λ4254	λ4255	λ4262	λ6334
87 Psc	5	—	13[a]	55[b]	44[b]
53 Tau	2	—	4	42[b]	8
μ Lep	46	20	68	85[b]	80
HR 2844	146[b]	50[b]	98	110[b]	136
κ Cnc	41	20	84	58[a]	118[a]
υ Her	16	8[a]	28	58[b]	35
ϕ Her	8	46[b]	10	67[b]	14
HR 6997	109[b]	22	67	58	97[a]
112 Her	22	9	35	32[a]	44
HR 7143	23	11	38	82[b]	44
HR 7361	41	20	72	65[a]	111
HR 7664	9	3	17	23[a]	22
HR 7775	13	6	19	72[b]	10
β Scl	17	26[b]	37	63[b]	—

[a]Blended 20–50%; [b]Blended >50%

4.2. Equivalent widths

We provide in Table 4 measured equivalent widths of the Ga II lines we have analysed by spectrum synthesis. These widths should be used cautiously, and are provided mainly as a guide to the strengths of the features. When equivalent widths refer to footnotes in Table 4, these indicate that the blending features are incorporated in the measurement and that we estimate that they contribute at least 20% of the total strength; in many cases the blends are dominant (>50%). Nearly all the other lines are blended to at least some degree. The least-blended lines are λ4251 and λ4255. Some comparisons with published equivalent widths (Ryabchikova et al. 1996; Adelman 1992; Adelman 1994) show that our results are in good agreement with these authors but diverge when one or the other set of measurements involves attempts to deblend the Ga II features via line fitting. This effect is seen particularly in λ4255, where our measurements include the Ga II λ4255.902 line and other weak blends, while Adelman and collaborators appear to have used deblending methods to exclude them when measuring.

5. Discussion

In view of the number of free parameters involved, it was not felt reasonable to assign a formal error to the fits for each line in each star. We formed the impression that, in the best cases of Ga-rich sharp-lined stars, the fitting errors were very small ($\Delta \log A = \pm 0.02$), while for more rapid rotators having lines with blending problems, the errors were of the order of $\pm$0.10-0.15 dex, in the sense that test syntheses with abundance variations of these magnitudes produced results that did not fit as well by eye as the values given in Table 3. Perhaps a better appreciation of the overall errors can be gathered from the values of σ, which include both fitting errors and scatter due to systematic differences in $\log gf$. These may be compared to the last line in the table, which gives the mean deviations of each line from the

individual mean optical abundances. These are of order ± 0.1, and represent, to a good approximation, the typical systematic differences. The abundances from the λ4251 and λ4254 lines are, on average, greater than the mean abundance whereas the abundances from the λ4255, λ4262 and λ6334 lines are less than the mean.

As can be seen from Table 3, the results from this analysis give gallium abundances that are only marginally greater than those that have been published for UV resonance lines, with a mean difference of only $+0.22 \pm 0.03$ dex, much less than that previously claimed for the discrepancy between the visible and UV lines. We note that Guthrie's (1984) differential curve-of-growth analysis took hyperfine structure into account and he derived results for several objects that do not differ greatly from those found here, although there are large differences in a few cases. Smith (1996a) indicated that one might account for a systematic difference of 0.1 dex by stratification effects. The remaining difference of 0.1 dex might be accounted for by possible systematic errors in optical *gf*–values, by fitting errors, and particularly by inadequacies in the simplified hfs that we adopted for the lines. Some preliminary tests with more detailed hfs theoretical models for the Ga II λ4255 line appear to indicate that this might account for the entire remaining 0.1 dex discrepancy. Future work should include consideration of complications due to the existence of two isotopes of Ga with somewhat different nuclear magnetic moments.

6. Conclusions

We defined the Gallium Problem as the apparent ~ 1 dex discrepancy, found by previous authors, between Ga abundances deduced from the UV and the visible lines. To investigate this problem, we have carried out a detailed LTE spectrum synthesis analysis of the visible-region lines of Ga II in a sample of HgMn stars for which there are also recent analyses of the Ga abundances based on UV resonance lines of Ga II and Ga III by Smith (1996a). The upper limit for detection of Ga from the high-excitation visible lines is ~ 2 dex higher than for the resonance lines, so that only those stars with strong Ga anomalies could be studied. We employed the set of *gf*–values of Ryabchikova & Smirnov (1994) and the observed hyperfine structures of Bidelman & Corliss (1962), or the Lanz et al. (1993) theoretical hyperfine structure for λ6334, to model the lines. We also took into account all known blending lines in an internally self-consistent fashion. One of the Ga II lines is severely affected by blending (λ4262) and none of the other lines can be correctly modelled without taking hyperfine structure into account.

The result found for the λ6334 line by Ryabchikova & Smirnov (1994) illustrates the Gallium Problem: without allowing for hyperfine structure, they found log A(Ga) = 8.48 from a measured equivalent width of 126 mÅ in κ Cnc and the same *gf*–value adopted here. Our much more accurate measured equivalent width (118 mÅ in Table 4) is similar to the one they used, so measurement error is not the source of the difference of 1.76 dex. When they made an allowance for hyperfine structure they obtained 7.34, leaving a difference of 0.62 dex. It is apparent from our results that part of this difference is due to their assumption that the line is unblended, whereas we find that this line is blended by Ne I, which adds about 20 mÅ to the observed equivalent width. The remaining difference is due to different adopted values for radiative and Stark damping parameters, which have a significant effect for this strong optical Ga II line.

We have shown that the Gallium Problem can be explained entirely in terms of incorrect allowance for these effects, or–in the case of the study of λ6334 by Lanz et al. (1993)–by the adoption of a radically different *gf*–value. The final resolution of the Gallium Problem for this line must await measurement of its oscillator strength. Nevertheless, the difference between the mean Ga abundance from visible-region lines and that from UV resonance lines is reduced to 0.22 dex under the assumption of homogeneous models, with a further reduction to ~ 0.12 dex if Ga is indeed stratified in the atmosphere along the lines proposed by Smith (1995). This remaining discrepancy is very likely explicable by the use of the rather crude hyperfine structure models we adopted.

Our basic conclusion is that the Gallium Problem may be solved by taking fully into account the hyperfine structures of the Ga II lines; this removes nearly all the discrepancies claimed in earlier work, and we conclude that there is no need for exotic explanations. There is an urgent need for an accurate laboratory oscillator strength for the λ6334 4s5s $^3S_1$–4s5p $^3P^\circ_2$ transition, as well as a need for a laboratory investigation of the hyperfine structure of the Ga II lines studied in this paper. In the meantime, further refinements should be possible by use of theoretical calculations of hfs, and we intend to investigate this.

Acknowledgements. We thank Dr. Keith C. Smith for helpful comments and for making available his unpublished Ga II hfs calculations. MMD is grateful to the Director of the University of California Observatories, Prof. J.S. Miller, for allocating time for his Guest Observer programme. Thanks also go to Mr Tony Misch and other technical and service staff at Lick Observatory, for their efforts on our behalf. We acknowledge the valuable comments of the referee, Dr. M.-C. Artru. Research on chemically peculiar stars at UCL is supported by PPARC grant GR/K58500. This work was also supported by the PPARC PATT Grant to UCL for travel to telescopes (GR/K60107). Claire Smith gratefully acknowledges support from an Undergraduate Research Bursary from The Nuffield Foundation, London (NUF-URB97) and the Frank Norman Jenkins Fund at University College London.

References

Adelman, S.J., 1992, MNRAS, 258, 167
Adelman, S.J., 1994, MNRAS, 266, 97
Allen, C.S., 1997, PhD Thesis, University of London
Anders, E., Grevesse, N., 1989, Geochim. Cosmochim. Acta, 53, 197
Andersen, T., Sørensen, G., 1972, Phys. Rev. A, 5, 2447
Ansbacher, W., Pinnington, E.H., Bahr, J.L., Kernahan, J.A., 1985, Can J Phys, 63, 1330
Bates, D.R., Damgaard, A., 1949, Phil. Trans A, 242, 101
Bidelman, W.P., Corliss, C.H., 1962, ApJ, 135, 968
Churchill, C.W., 1995, Lick Obs. Tech. Rep. No. 74
Cugier, H., Hardorp, J., 1988, A&A, 197, 163

Dimitrijević, M.S., Artru, M.-C., 1986, In: Kurepa, M.V. (ed.) The Physics of Ionized Gases, XIII SPIG, University of Beograd, p. 317
Griem, H.R., 1968, Phys Rev, 165, 258
Guthrie, B.N.G., 1984, MNRAS, 206, 85
Isberg, B., Litzen, U., 1985, Phys Scr, 31, 533
Jugaku, J., Sargent, W.L.W., Greenstein, J.L., 1961, ApJ, 134, 783
Kurucz, R.L., 1990, Transactions of the International Astronomical Union XXB, 168
Lanz, T., 1995, In Astrophysical Applications of Powerful New Databases, Adelman S.J., Wiese, W.L. (eds.), PASPC No. 78, p. 423
Lanz, T., Artru, M.-C., Didelon, P., Mathys, G., 1993, A&A, 272, 465
Misch, A. 1995 (priv. comm.)
Misch, A., 1997, User's Guide to the Hamilton Echelle Spectrometer, URL=http://www.ucolick.org/~tony/instruments/hamspec/hamspec_index.html
Ryabchikova, T.A., Smirnov, Yu. M., 1994, Astronomy Reports, 38, 1
Ryabchikova, T.A., Zakhorova, L.A., Adelman, S.A., 1996, MNRAS, 283, 1115
Smalley, B., 1996 (priv.comm.)
Smith, K.C., 1992, PhD thesis, University of London
Smith, K.C., 1995, A&A 297, 237
Smith, K.C., 1996a, A&A 305, 902
Smith, K.C., 1996b, Ap&SS 237, 77
Smith, K.C., Dworetsky, M.M., 1988, In: Adelman, S.J., Lanz, T. (eds) Elemental Abundance Analyses. Institut d'Astronomie de l'Univ. de Lausanne, Switzerland, p. 32
Smith, K.C., Dworetsky, M.M., 1993, A&A 274, 335
Takada-Hidai, M., Sadakane, K., Jugaku, J., 1986, ApJ, 304, 425
Valdes, F., 1990, The IRAF APEXTRACT Package, URL=ftp://iraf.tuc.noao.edu/iraf/docs/apex.ps
Vauclair, S., Vauclair. G., 1982, ARA&A 20, 37
Vogt, S., 1987, PASP, 99, 1214
Warner, B., 1967, MNRAS, 136, 381